

doi:10.3969/j.issn.1672-4623.2021.11.015

基于MODIS数据的黄河源区植被覆盖度反演研究



刘晶¹, 党星海^{1,2}, 陈丽丽¹, 边雁君³, 黄立鑫¹, 李志红¹, 周兆叶^{1*}

(1. 兰州理工大学 土木工程学院, 甘肃 兰州 730050; 2. 甘肃省应急测绘工程研究中心, 甘肃 兰州 730050;
3. 中铁二十局集团市政工程有限公司, 甘肃 兰州 730030)

摘要: 以黄河源区高寒草地为研究对象, 采用无人机航拍技术获取了样地实测的植被覆盖度; 结合2001—2018年MODIS13A1数据提取常用植被指数, 分别采用像元二分模型法和回归模型法对研究区植被覆盖度进行了反演, 并对其精度进行了验证; 采用最小二乘法分析了黄河源区2001年以来植被覆盖度的变化趋势。结果表明, 修正的土壤调节植被指数结合回归模型的反演精度较高; 黄河源区多年平均植被覆盖度为57.89%, 植被覆盖度处于30%以内、30%~60%、60%以上3个区间的面积分别占源区总面积的13.1%、27.25%和49.65%; 2001—2018年黄河源区植被覆盖度略呈增长趋势。

关键词: 无人机航拍; 黄河源区; 植被指数; 植被覆盖度; 反演; 最小二乘法

中图分类号: P237

文献标志码: B

文章编号: 1672-4623(2021)11-0057-06

高寒草地是维持高原地区生态平衡的关键物种, 高寒草地的退化将导致不可逆转的生态问题, 因此对于高寒草地的监测至关重要。高寒草地的监测方法主要包括传统的地面调查和利用植被指数进行遥感估测^[1], 地面调查方法费时费力, 样本数量少, 空间代表性差, 得出的结论不足以很好地反映高寒草地覆盖度的真实空间分布状态^[2-3]; 遥感估测的常用手段包括卫星遥感、无人机遥感等^[4]。利用无人机能低空飞行、悬停等特点进行取样^[5-6], 并配合少量地面取样, 可成为样方尺度高寒草地覆盖度、高度、生物量调查的主要手段, 在很大程度上解决传统观测方法的不足^[7-8]。无人机操作灵活, 可通过设置其飞行高度和飞行模式获取与遥感像元尺度匹配的图像, 能架起样地实测数据与遥感影像之间的桥梁。目前基于植被指数的遥感估测方法包括回归方程法、像元二分法和机器算法等^[1,7]。

本文以黄河源区的高寒草地为研究对象, 以无人机航拍为获取数据的主要手段, 结合地面样方调查数据和MODIS数据提取了植被指数; 再利用回归模型法和像元二分法反演了源区高寒草地覆盖度; 最后筛选最优指数和算法进行黄河源区高寒草地覆盖度估算以及变化趋势分析, 以期高寒草地的合理利用与生态治理提供数据支撑。

1 数据来源与研究方法

1.1 数据来源

1.1.1 研究区概况与数据获取

本文所指的黄河源区为唐乃亥水文站以上区域, 面积为 $1.2 \times 10^5 \text{ km}^2$, 主要植被类型为高寒草地、高寒灌丛化草地和高寒草甸等^[8-9]。该区域植被生长季节性变化明显, 对气候变化极其敏感, 属于生态脆弱带和气候变化敏感区^[10-12]。

本文采用大疆精灵 Pro 四旋翼无人机, 航高设置为20 m, 样地大小布设为 $250 \text{ m} \times 250 \text{ m}$ (以便与MODIS数据像元大小匹配), 样地内以矩形的方式获取照片, 每块样地共获取13张照片, 单张照片覆盖范围约为 $35 \text{ m} \times 35 \text{ m}$ ^[3]。2016—2018年7月底8月初在黄河源区共拍摄326块样地, 4 238张照片。样地位置分布如图1所示。

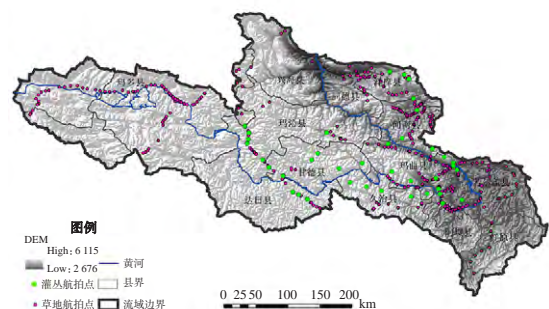


图1 研究区航拍样地位置分布

收稿日期: 2020-06-09。

项目来源: 甘肃省自然科学基金资助项目(20JR5RA444); 国家自然科学基金资助项目(51968042)。

(* 为通信作者)

1.1.2 MODIS 数据下载

根据黄河源区的经纬度范围，确定行列号为 h25v05、h26v05 的两景数据可覆盖全区域。该数据的时间分辨率为 16 d，空间分辨率为 500 m。本文下载数据时间序列为 2001—2018 年 7 月 11 日（以便与野外航拍时间一致）的 MOD11A1 和 MOD13A1 数据，共 72 景影像。

1.2 研究方法

无人机样地植被覆盖度采用项目团队自主开发的覆盖度提取软件进行计算。首先利用 MODIS Tool 软件对下载的源区 MOD13A1 数据进行预处理，包括定义投影、裁切等，并提取、计算得到归一化植被指数 (NDVI)、增强型植被指数 (EVI)、土壤调节植被指数 (SAVI) 和修正的土壤调节植被指数 (MSAVI)^[3]；然后利用回归模型法和像元二分模型，分别基于 4 种植被指数对黄河源区植被覆盖度进行反演，并比较各植被指数采用上述两种方法的反演精度；最后比较采用同种反演方法，哪种植被指数的反演精度更高就采用该植被指数进行逐年反演，并分析黄河源区 2001—2018 年植被覆盖度的变化情况。

2 黄河源区植被覆盖度反演

2.1 黄河源区样地植被覆盖度提取

本文采用研究团队自主开发的 Pixel Based Manual Classifier V1 软件提取航拍照片的植被覆盖度和非植被等

信息。该软件能利用阈值法快速、高效、准确地区分植被和非植被，并根据分类结果进行植被覆盖度的计算。

2.2 植被覆盖度反演

2.2.1 植被指数数据获取

首先从经过预处理的 MOD13A1 数据中提取 NDVI、EVI，再提取红光波段和近红外波段，用以获取 SAVI 和 MSAVI^[4]。

2.2.2 基于植被指数的回归模型法

基于植被指数的回归模型法首先建立植被指数与实测植被覆盖度的关系，再结合卫星遥感数据将该关系反推到整个黄河源区，从而获得黄河源区的植被覆盖度数据。

本文首先分别计算 2001—2018 年各种植被指数的均值，再采用“提点法”得到各植被指数的像元值，并利用其中 75% 的样本点数据与植被覆盖度建立拟合关系，然后通过拟合关系进行反演，最后利用 25% 的样本点进行验证，比较其反演精度。

1) 利用 75% 的植被覆盖度对各植被指数均值进行采样，并建立植被指数与实测植被覆盖度之间的散点图，得到拟合关系式，如图 2 所示。

2) 在 ArcGIS 中，分别利用各植被指数的拟合关系式反演整个黄河源区的植被覆盖度，结果如图 3 所示。

3) 利用剩余的 25% 的样本点数据进行精度验证，结果如图 4 所示。

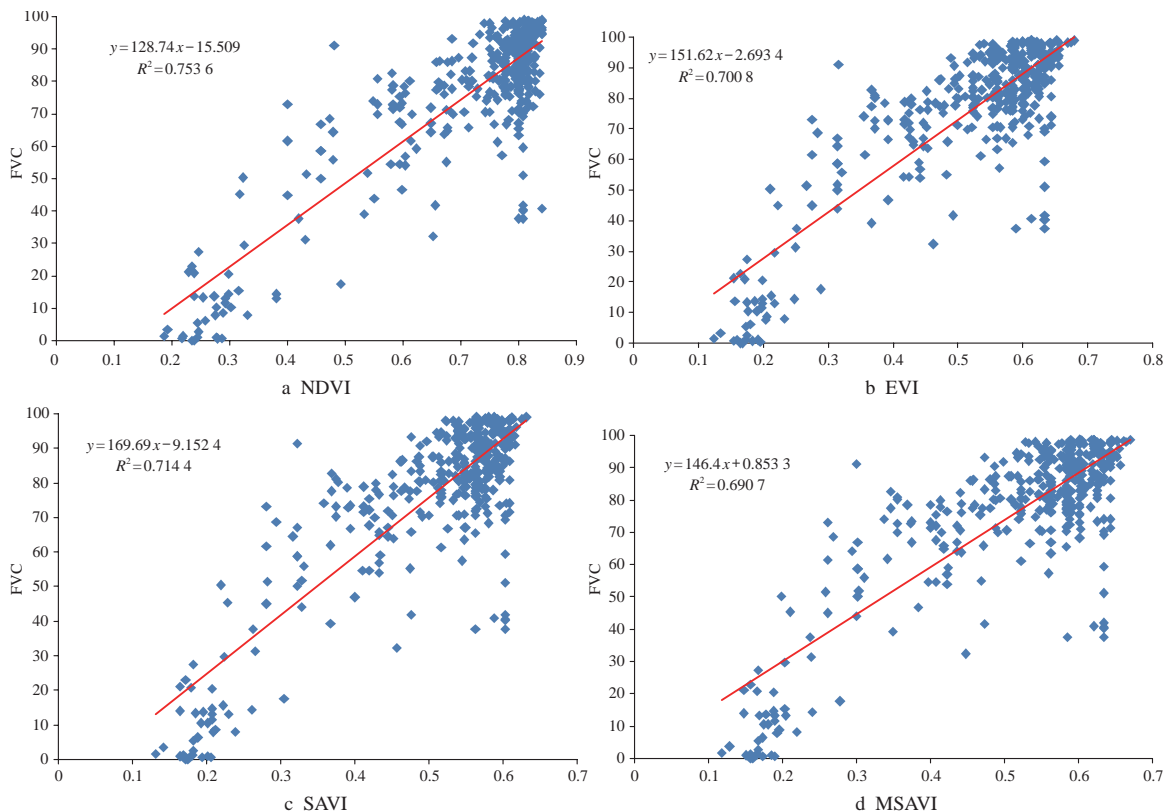


图 2 植被指数与实测 FVC 建立的拟合关系

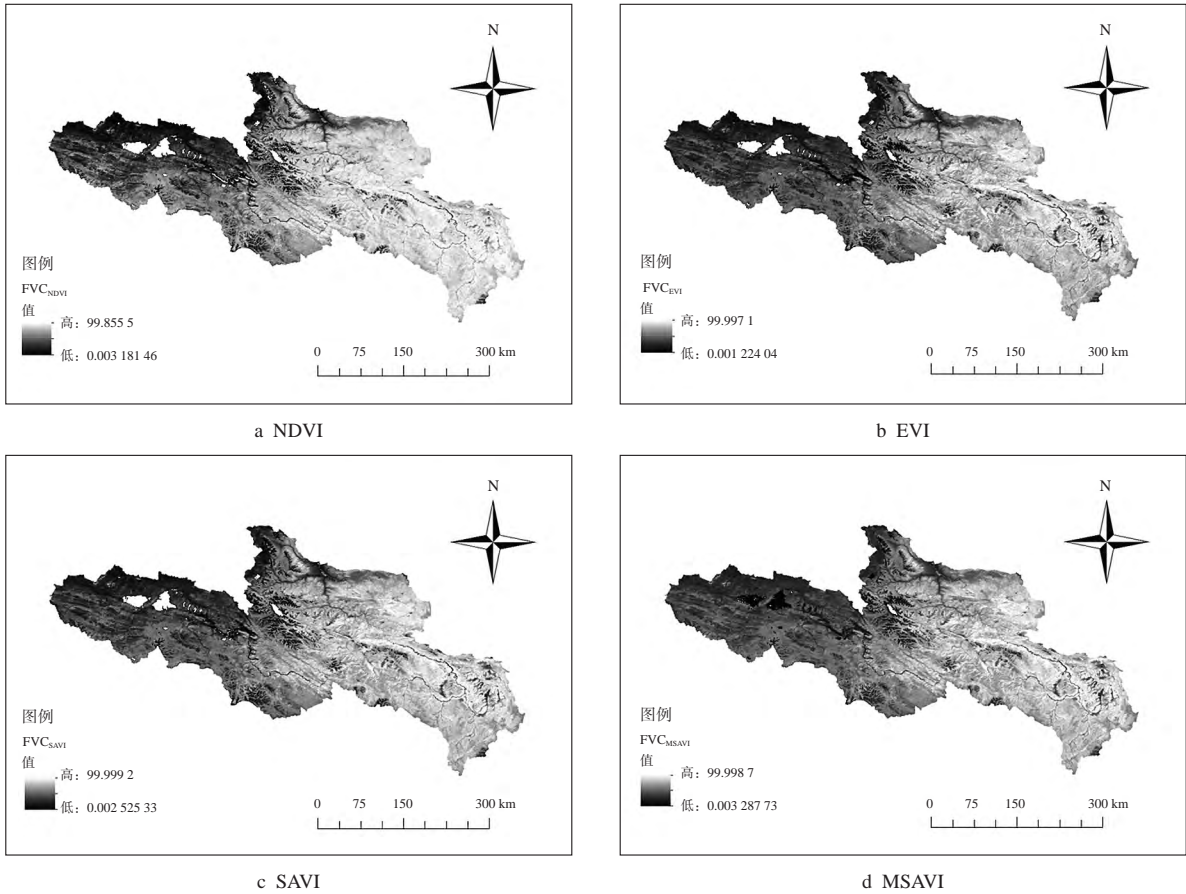


图3 回归模型法各植被指数的反演结果

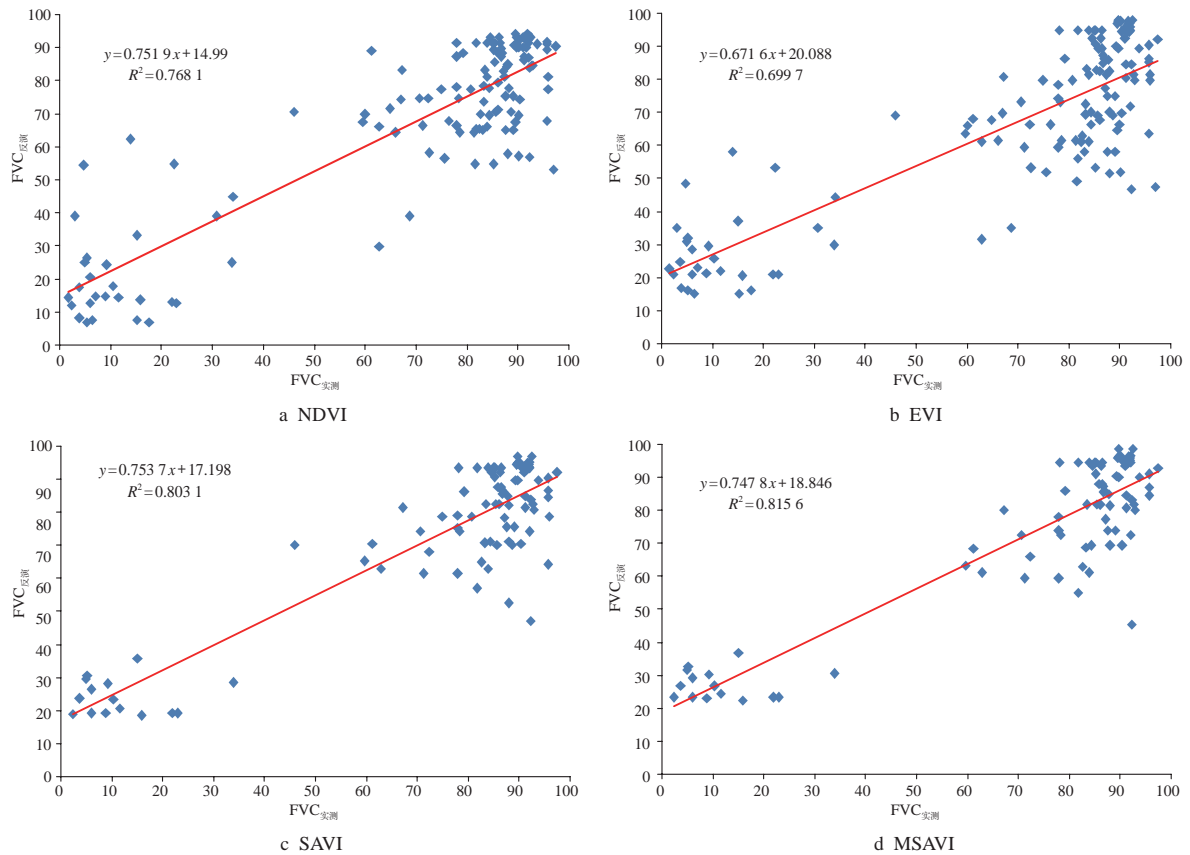


图4 回归模型法精度验证

2.2.3 像元二分模型法

像元二分模型法是将像元中的地物组成分为植被与非植被两部分，通过获取纯植被像元与非纯植被像元的光谱信息来达到分解混合像元的目的。通过分解可计算得到该混合像元中植被因子所占的比例。以 NDVI 为例，植被覆盖度的计算公式为：

$$FVC = (NDVI - NDVI_{soil}) / (NDVI_{veg} - NDVI_{soil})$$

式中， $NDVI_{soil}$ 为纯土壤像元对应的 NDVI 值； $NDVI_{veg}$ 为纯植被像元对应的 NDVI 值；NDVI 为需要计算植被覆盖度的混合像元的 NDVI 值。

$$NDVI_{soil} = (FVC_{max} \times NDVI_{min} - FVC_{min} \times NDVI_{max}) / (FVC_{max} - FVC_{min})$$

$$NDVI_{veg} = ((1 - FVC_{min}) \times NDVI_{max} - (1 - FVC_{max}) \times NDVI_{min}) / (FVC_{max} - FVC_{min})$$

具体取值方法为：若有实测数据，则分别取实测植被覆盖度的最大值和最小值作为 FVC_{max} 和 FVC_{min} ，遥感影像中的 NDVI 值作为 $NDVI_{max}$ 和 $NDVI_{min}$ ，与实测的 FVC_{max} 和 FVC_{min} 数据相对应^[6]。

与回归模型法一样，采用 75% 的样本点进行计算，25% 的样本点进行精度验证，拟合结果如图 5 所示。结合样地所在像元拟合得到的植被覆盖度与样地实测植被覆盖度进行精度验证，结果如图 6 所示。

2.3 逐年反演植被覆盖度

两种方法精度验证的相关系数如表 1 所示，可以

看出，对于 4 种植被指数来说，回归模型法的模拟精度均优于像元二分模型法；对于回归模型法来说，4 种植被指数中 MSAVI 的反演精度最高， R^2 达到了 0.815 6。因此，本文采用回归模型结合 MSAVI 建立的关系： $y = 146.4x + 0.853 3$ ，作为反演 2001—2018 年黄河源区植被覆盖度的依据。

表 1 两种方法精度验证的相关系数 R^2

方法	NDVI	EVI	SAVI	MSAVI
回归模型法	0.768 1	0.699 7	0.803 1	0.815 6
像元二分模型法	0.596 3	0.538 4	0.558 6	0.518 5

3 研究结果分析

3.1 2001—2018 年植被覆盖度变化分析

本文采用最小二乘线性回归模型计算黄河源区 2001—2018 年植被覆盖度的变化情况。该方法常用于分析长时间序列的植被变化趋势，将时间变量 t 作为独立变量，与各年的 NDVI 时序数据进行最小二乘回归分析，从而得到一个线性方程；再利用该方程，根据其斜率数值，获得源区 2001—2018 年植被覆盖度的变化趋势。若斜率小于零，则植被生长呈下降趋势；反之，则呈增长趋势。时间变化公式为：

$$y = a + bx$$

式中， y 为各年的平均植被覆盖度； a 为拟合参数； b 为线性回归方程的斜率^[6]。

2001—2018 年黄河源区植被覆盖度变化趋势如

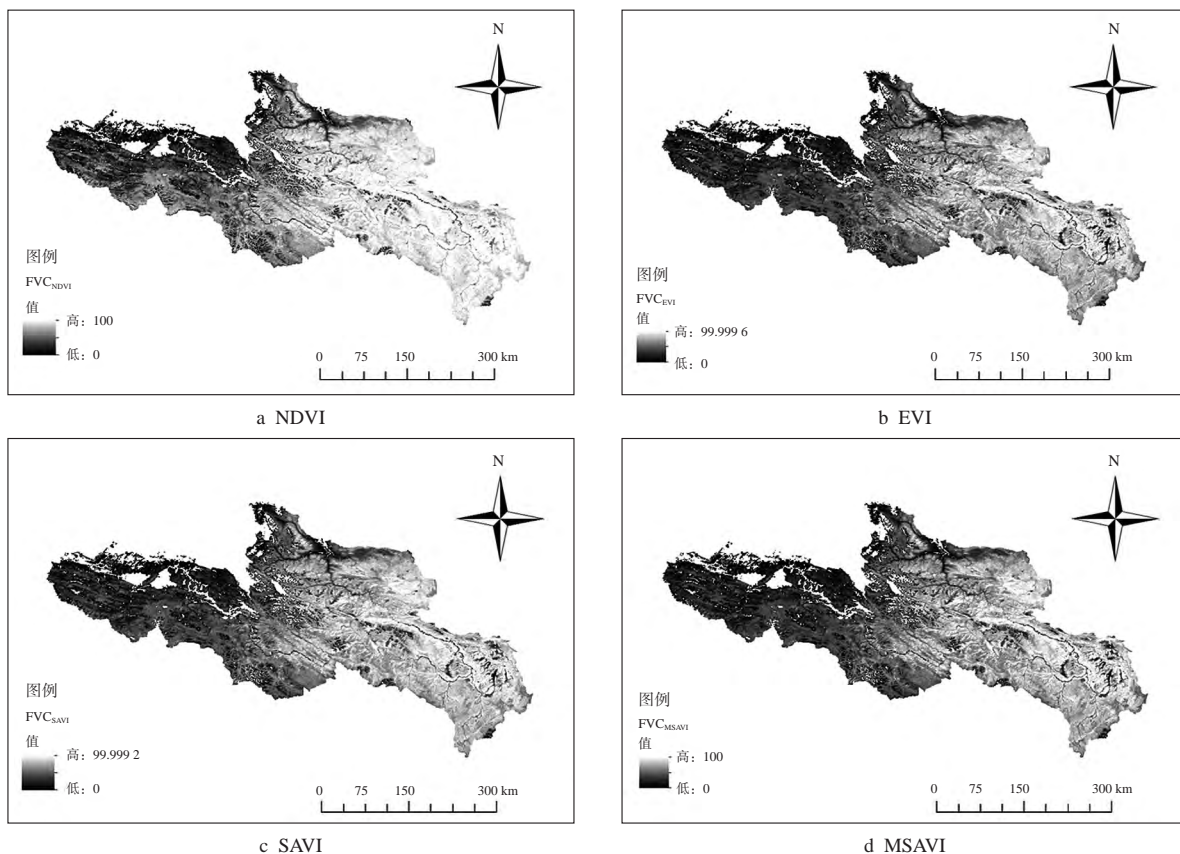


图 5 像元二分模型法各植被指数反演结果

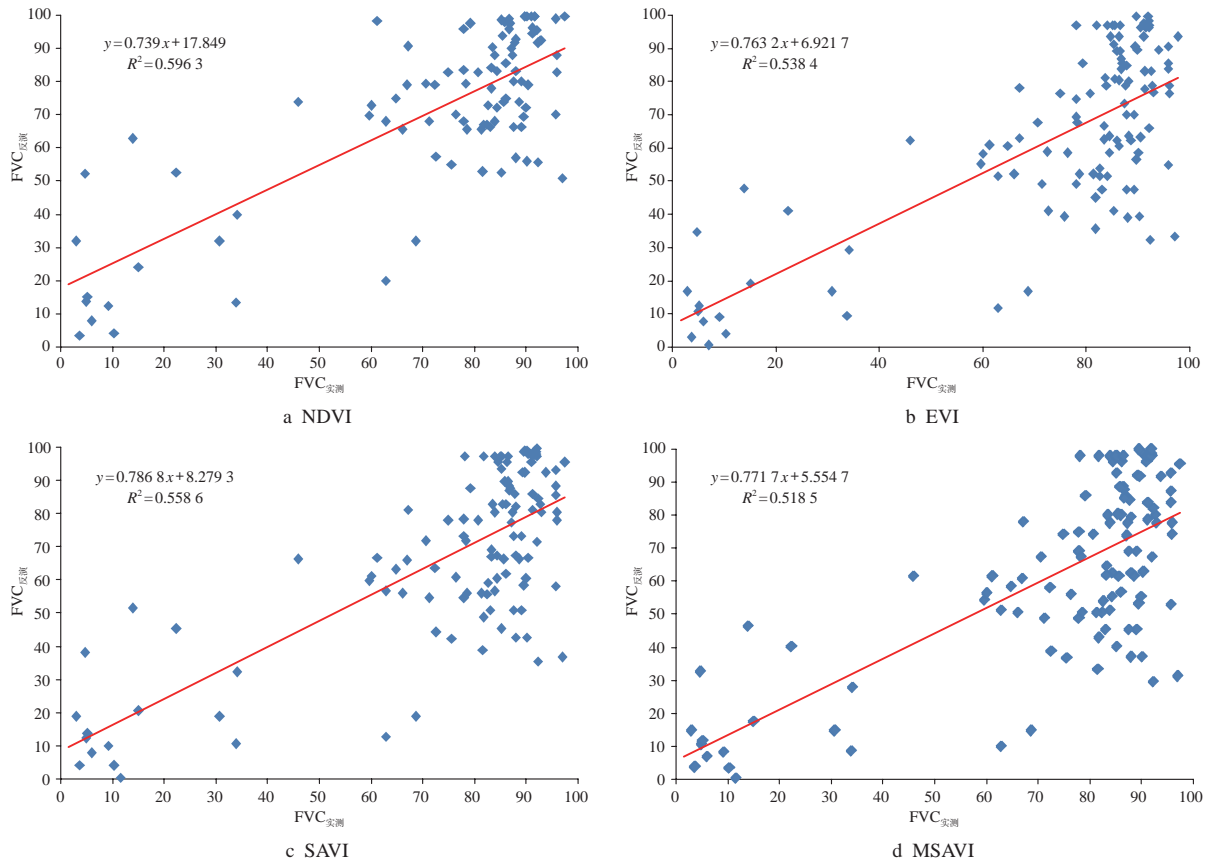


图6 像元二分模型法精度验证

图7所示，可以看出，2001—2018年源区的植被覆盖度整体呈增长趋势，但增长不是很明显，且自2001年以来，黄河源区植被覆盖度在50%~70%之间。

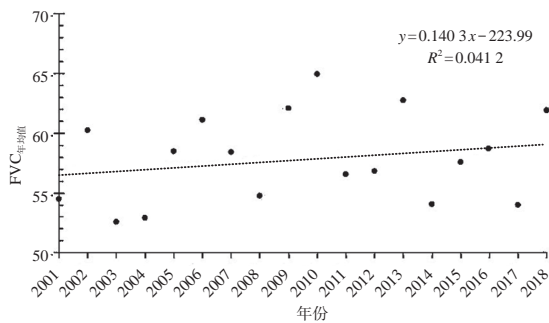


图7 2001—2018年黄河源区植被覆盖度变化趋势分析

3.2 黄河源区多年植被覆盖度均值统计分析

本文根据植被覆盖度划分标准(表2)对黄河源区植被覆盖度多年均值进行分级^[13-14]，结果如图8所示，并统计了不同覆盖度等级所占的比例(表3)。

结合图8和表3可知，整个黄河源区内植被覆盖度<10%的裸地，占比为1.41%；植被覆盖度为10%~30%的低覆盖区，占比为11.69%；植被覆盖度为30%~45%的中低覆盖区，占比为17.66%；植被覆盖度为45%~60%的中覆盖区，占比为19.59%；植被覆盖度>60%的高覆盖区，占比为49.65%；因此黄河源区约50%的地区其植被覆盖度在60%以上。

表2 植被覆盖度划分标准

等级	划分标准
裸地	< 10%
低覆盖	10% ~ 30%
中低覆盖	30% ~ 45%
中覆盖	45% ~ 60%
高覆盖	> 60%

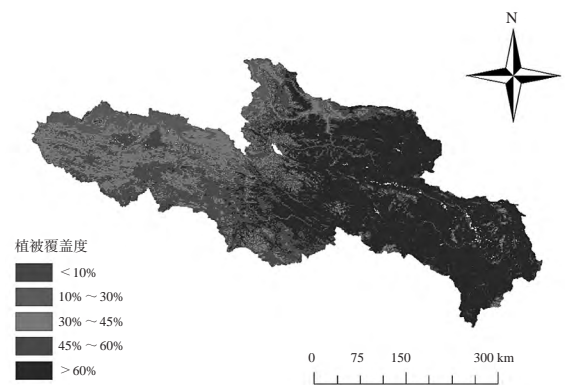


图8 黄河源区植被覆盖度分级结果

表3 黄河源区植被覆盖度不同等级的面积统计

植被覆盖度	面积/km ²	占比/%
< 10%	2 015.25	1.41
10% ~ 30%	16 681	11.69
30% ~ 45%	25 198	17.66
45% ~ 60%	27 947.5	19.59
> 60%	70 848.5	49.65

4 结 语

1) 2001—2018 年黄河源区的植被覆盖度整体呈增长趋势, 但该趋势不是很明显, 且自 2001 年以来, 黄河源区植被覆盖度在 50% ~ 70% 之间。

2) 整个黄河源区内植被覆盖度 < 10% 的裸地, 占比为 1.41%; 植被覆盖度为 10% ~ 30% 的低覆盖区, 占比为 11.69%; 植被覆盖度为 30% ~ 45% 的中低覆盖区, 占比为 17.66%; 植被覆盖度为 45% ~ 60% 的中覆盖区, 占比为 19.59%; 植被覆盖度 > 60% 的高覆盖区, 占比为 49.65%; 因此, 黄河源区约 50% 的地区其植被覆盖度在 60% 以上。

本文只选用了 MODIS 数据进行研究, 没有结合其他较长时间序列数据 (如 GIMMS) 进行长时间序列的黄河源区植被覆盖度的变化趋势分析; 计算得到了黄河源区 2001—2018 年的植被覆盖度变化趋势, 但未进行影响因素分析, 这也是今后需继续研究的内容。

参考文献

[1] CHEN J, YI S H, QIN Y, et al. Improving Estimates of Fractional Vegetation Cover Based on UAV in Alpine Grassland on the Qinghai-Tibetan Plateau[J]. *International Journal of Remote Sensing*, 2016, 37(8): 1 922-1 936

[2] YI S H, ZHOU Z Y, REN S L, et al. Effects of Permafrost Degradation on Alpine Grassland in a Semi-arid Basin on the Qinghai-Tibetan Plateau[J]. *Environmental Research Letters*, 2011(6): 45-55

[3] ZHOU Z Y, YI S H, CHEN J, et al. Response of Alpine Grassland

to Climate Warming and Permafrost Thawing in Two Basins with Different Precipitation Regimes on the Qinghai-Tibetan Plateau[J]. *Arctic, Antarctic and Alpine Research*, 2015, 47(1): 125-131

[4] 董洲, 赵霞, 梁栋, 等. 内蒙古灌丛化草原分布特征的遥感辨识[J]. *农业工程学报*, 2014, 30(11): 152-158

[5] 李德仁, 李明. 无人机遥感系统的研究进展与应用前景[J]. *武汉大学学报(信息科学版)*, 2014, 39(5): 505-513

[6] 姬渊, 秦志远, 王秉杰, 等. 小型无人机遥感平台在摄影测量中的应用研究[J]. *测绘技术装备*, 2008(1): 46-48

[7] ZHANG H F, SUN Y, CHANG L, et al. Estimation of Grassland Canopy Height and Aboveground Biomass at the Quadrat Scale Using Unmanned Aerial Vehicle[J]. *Remote Sensing*, 2018(10): 851-855

[8] CHEN J, YI S H, QIN Y. The Contribution of Plateau Pika Disturbance and Erosion on Patchy Alpine Grassland Soil on the Qinghai-Tibetan Plateau: Implications for Grassland Restoration[J]. *Geoderma*, 2017(297): 1-9

[9] 徐浩杰, 杨太保, 曾彪. 黄河源区植被生长季 NDVI 时空特征及其对气候变化的响应[J]. *生态环境学报*, 2012, 21(7): 1 205-1 210

[10] 宋翔, 颜长珍, 朱艳玲, 等. 黄河源区土地利用/覆被变化及其生态环境效应[J]. *中国沙漠*, 2009, 29(6): 1 049-1 055

[11] 李开明, 李绚, 王翠云, 等. 黄河源区气候变化的环境效应研究[J]. *冰川冻土*, 2013, 35(5): 1 183-1 192

[12] 马天啸, 宋现锋, 赵昕, 等. 2000—2010 年黄河源区植被覆盖率时空变化及其影响因素[J]. *干旱区研究*, 2016, 33(6): 1 217-1 225

[13] 叶姣琬, 何政伟, 翁中银, 等. NDVI 像元二分模型在喀斯特地区提取石漠化中的应用[J]. *地理空间信息*, 2012, 10(4): 134-136

[14] 张宇婷, 张振飞, 张志. 新疆大南湖荒漠区 1992—2014 年间植被覆盖度遥感研究[J]. *国土资源遥感*, 2018, 30(1): 187-195

第一作者简介: 刘晶, 硕士研究生, 研究方向为无人机航拍与环境遥感。

(上接第 56 页)

4 结 语

本文利用 PS-InSAR 方法对覆盖个旧市的 23 景 Sentinel-1A 卫星数据进行了处理, 获得了该地区 2018-03-22—2019-01-16 的地表形变信息。研究表明, 该地区的沉降速率在 -49.89 ~ 25.52 mm/a 之间, 沉降严重的区域与锡矿开采区基本一致, 而个旧市城区地质条件稳固、形变量较小。PS-InSAR 方法能对该地区的地表进行监测, 有效减少了人力物力成本; 但 InSAR 技术也存在一些缺陷, 如植被茂密地区干涉信号失相干严重。今后还需结合 GNSS、水准测量等多种技术手段, 合理利用各种测量方法的优势, 对该地区地表沉降进行有效监测, 以便能更好地为该地区的灾害防治提供技术支撑。

参考文献

[1] Sanaz V, Mahdi M, Faramarz N. StaMPS Improvement for

Deformation Analysis in Mountainous Regions: Implications for the Damavand Volcano and Mosha Fault in Alborz[J]. *Remote Sensing*, 2015, 7(7): 8 323-8 347

[2] 罗想, 王萍, 张艳梅, 等. 基于 SBAS 时序分析方法的断裂带形变监测[J]. *地理空间信息*, 2018, 16(3): 114-116

[3] Ferretti A, Prati C, Rocca F. Permanent Scatterers in SAR Interferometry[J]. *IEEE Transactions on Geoscience and Remote Sensing*, 2001, 39(1): 8-20

[4] 廖丽. 锡都个旧的兴衰[M]. 昆明: 云南教育出版社, 2013

[5] Sentinel-1 Team. Sentinel-1 User Handbook[M]. European Space Agency, Paris, 2013

[6] Hooper A, Segall P, Zebker H. Persistent Scatterer InSAR for Crustal Deformation Analysis, with Application to Volcán Alcedo, Galápagos[J]. *Journal of Geophysical Research*, 2007, 112(B07407): 19

[7] 李少青, 杨武年, 杨彦通, 等. Sentinel-1A_IW 雷达影像在地震形变信息提取中的应用[J]. *测绘*, 2016, 39(2): 56-59

[8] 吴文豪. 哨兵雷达卫星 TOPS 模式干涉处理研究[D]. 武汉: 武汉大学, 2016

第一作者简介: 马丽, 工程师, 从事土地测绘、不动产登记、土地储备、土地资源管理等工作。

Research on Automatic Extraction Method of Route Sectional Data of Broken Terrain

by CHANG Junfeng

Abstract In view of the present situation of high labor intensity, low efficiency and poor data accuracy in the conventional route sectional measurement in the broken terrain, we proposed a new method based on Visual LISP language for constructing irregular triangular network to automatically extract sectional data in the broken terrain. The practical engineering application shows that this method can greatly improve the extraction efficiency of sectional data, and has certain practical value in production.

Key words broken terrain, cross-section measurement, irregular triangular network (Page: 38)

Research on Intelligent Linefeed Method of Map Annotation with Considering Semantics

by ZHANG Wei

Abstract In this paper, we proposed an intelligent linefeed method of map annotation with considering semantics. The method can solve the problems that the long annotations in the Internet map are not beautiful and the manual work is heavy, and improve the readability of map annotation. This method has been used in the electronic map production of "MapWorld · Fujian", and plays an important role.

Key words map annotation, point of interest, jieba parteciple, FME (Page: 41)

Positioning Performance Analysis of BDS-2/BDS-3 Short Baseline RTK at Different Altitude Angles

by LUO Jie

Abstract Aiming at the current BDS positioning performance evaluation problem, we analyzed the short baseline RTK positioning performance of BDS-2, BDS-3 and BDS-2/BDS-3 at different altitude angles based on the short baseline data of about 12.93 km composed of domestic MGEX. The experimental results show that as the altitude angle increases, the number of satellites available, positioning accuracy and epoch rate of BDS-2 and BDS-3 decrease significantly, and the PDOP value increases significantly. While BDS-2/BDS-3 can effectively improve this situation, make up for the poor positioning performance of single satellite in extreme environments, and provide a certain reference for future BDS positioning performance research.

Key words BDS, different altitude angles, RTK, accuracy (Page: 44)

Wetland Landscape Pattern Evolution and Its Driving Force Analysis in Zhuhai City

by YU Lin

Abstract Wetland ecosystem is one of the three major ecosystems in the world. It provides the living environment for 20% of the known species on earth and enjoys the reputation of "kidney of the earth". However, under the background of rapid urban development, the wetland ecosystem has encountered a major threat. In this paper, taking the ecosystem of Zhuhai City as the research object, we interpreted the spatial distribution of wetland landscape pattern in Zhuhai City based on Sentinel-2 remote sensing images with a resolution of 10 m from 2016 to 2019. Then, we used ArcGIS spatial analysis and Fragstats methods to calculate its landscape pattern indexes, and analyzed the changes of wetland landscape pattern in Zhuhai City and its driving factors. The results show that ①reservoir and pit are the dominant landscape types of wetland landscape in Zhuhai City. Among them, the fragmentation degrees of pits, lakes, marshes and wetlands are increasing, and the spatial connectivity is poor. The aggregation degrees of river and mangrove forest are relatively good. ②The wetland area in Zhuhai City decreased year by year from 2016 to 2019, and the total decrease area reached 1 656.66 hm². Among them, the area decreased the most for pit surface and marsh wetland, and the area increased the most for mangrove woodland wetland. ③The reduction of pit and marsh wetlands are mainly due to the diversion of non-wetland, while the phenomenon of non-wetland diversion is relatively rare. ④The main factor leading to the reduction of wetland landscape in Zhuhai City is the rapid economic development. The expansion of population and the development of fishery also threaten the wetland.

Key words wetland ecosystem, landscape pattern, driving factor, Zhuhai City (Page: 48)

Surface Deformation Monitoring in Gejiu City Based on PS-InSAR Technique

by MA Li

Abstract In this study, based on 23 Sentinel-1A satellite images of Gejiu City from March 22, 2018 to January 16, 2019, we used PS-InSAR

technique to process these images, and acquired the surface deformation characteristics in Gejiu City. The result shows that the mean surface deformation rate in this area is from -49.89 mm/a to 25.52 mm/a. The tin mining area is the area with serious subsidence. The geologic conditions of Gejiu City are relatively stable and the deformation quantity is small.

Key words surface deformation, Sentinel-1A, PS-InSAR, Gejiu City (Page: 54)

Research on Inversion of Vegetation Coverage in Source Region of Yellow River Based on MODIS Data

by LIU Jing

Abstract Taking the alpine grassland of the Yellow River source area as the research object, we used the UAV aerial photography technology to obtain the measured vegetation coverage of the sample, and combining with the MOD13A1 data from 2001 to 2018, extracted the common vegetation index. And then, we used the pixel dichotomy model method and regression model method to invert the vegetation coverage in the study area, and verified its accuracy. Finally, we used least squares method to analyze the change trend of vegetation coverage in source area since 2001. The results show that the modified soil regulatory vegetation index combined with the regression model has a higher accuracy. The average annual vegetation coverage of source area is 57.89%. The area proportions with vegetation coverage within 30%, 30% ~ 60% and above 60% are 13.1%, 27.25% and 49.65% of the source area, respectively. The vegetation coverage in source area shows a slight increase from 2001 to 2018.

Key words UAV aerial photography, the Yellow River source area, vegetation index, FVC, inversion, least square method (Page: 57)

Fast Vectorization Method for Paper Map with Geographical Coordinate Recognition

by YANG Yang

Abstract In the process of manual vectorization of raster image based on scanning of traditional paper map, it needs the coordinate conversion of vector data, which is time-consuming and labor-intensive, and the accuracy is often affected by subjective factors. In order to achieve fast and accurate vectorization, we put forward a fast vectorization method for paper map with geographical coordinate recognition in this paper. We used the scanning raster images and latitude and longitude template to perform SURF feature matching, and obtained the latitude and longitude identity information and the corresponding horizontal ordinate information at first. And then, we calculated affine transform model parameters, and realized the transformation from pixel coordinates to geographical coordinates in the vectorization process. Experimental results show that this method can not only realize the vectorization of raster image, but also accurately complete the coordinate transformation of vector data, which can improve the vectorization efficiency of paper map.

Key words SURF, feature match, vectorization, run length code (Page: 63)

Control Measurement and Coordinate Transfer in Automatic Monitoring of Total Station

by WANG Weicai

Abstract In the automatic monitoring methods of total station used in the rail transit operation line, the measurement station is often located in the deformation area, so the coordinates of the measurement station need to be calculated in real time. At this time, it is often necessary to judge whether the accuracy of the two coordinates is the same and whether it is necessary to adopt new coordinate values? Due to the narrow space and limited requirements in the tunnel, the objective conditions of control network layout are greatly limited. It is necessary to carry out experimental analysis of the applications of some control measurement methods in the tunnel. In this paper, we discussed the control network design, the coordinate transfer and inspection of total station automatic monitoring method in tunnel.

Key words automatic total station, control network, coordinate transfer, inspection, Helmert (Page: 66)

Spatio-temporal Variations Analysis of Land Coverage Types and Urban Heat Island for Yangtze River Delta

by XIONG Xiaofeng

Abstract Based on the land surface temperature (LST) and land coverage data of MODIS, taking the Yangtze River Delta (YRD) as study area, we studied the spatio-temporal variations of land cover and urban heat